International Journal of Bridge Engineering (IJBE), Vol. 10, No. 2, (2022), pp. 37-59

EFFECTS OF ELASTOMER HARDNESS AND FRICTION COEFFICIENT ON DECK UNSETTLING SAFETY IN QUASI-ISOLATED BRIDGES

Mohammad Barkhordary, Saied Tariverdilo and Afshin Movaffaghi

Urmia University, Urmia, Iran.
e-mail: md.barkhordary@gmail.com, s.tariverdilo@urmia.ac.ir, movaffaghi.ac.ir@gmail.com

ABSTRACT: Using thermal elastomeric bearings, reinforced with thin steel shims and without thick ends plates and no bending requirements in quasi-isolation design, instead of conventional seismic isolators, potentiate bridge deck to slid on its bearings during moderate to strong earthquakes. Employing potential of that fusing mechanism between substructure and superstructure which could dissipate energy through friction is called quasi isolation system. However, as quasi-isolation design benefits from that sliding, deck displacement pushes the bridge toward deck unsetting as an extreme unacceptable damage. Interestingly, the elastomeric bearing sliding behavior affected strongly by bearing geometric and elastomeric material hardness. Although, friction coefficient between elastomeric material and bearing concrete seat has been studied in many previous literatures but, consideration effects of elastomeric material hardness and some special bearing geometry on quasi isolated bridges, haven't been studied till this paper. This study shows the elastomer hardness, bearing geometry and friction coefficient (*CoF*) effect on deck unsetting safety, which may violate current support length calculations.

KEYWORDS: quasi-isolation, bridge, earthquake, friction coefficient, elastomer hardness, unsetting

1 INTRODUCTION

The quasi isolated bridge design method is a new concept in bridge retrofit and design which developed after AASHTO increased the bridges seismic design return period from 500 years to 1000 years in 2008 (Bridges 2011). This increase caused additional seismic demands on under-design bridges and, many existing bridges categorized as retrofit needs. As an economical response, Illinois Department of Transportation (IDOT) in collaboration with the Illinois Centre of Transportation (ICT) conducted a study that compared a series of experimental and analytical research to find out usability and feasibility of applicability of its special thermal elastomeric bearing instead of elastomeric seismic isolators and also to improve its pre-defined earthquake resistance strategy (IDOT-ERS)

(Tobias et al. 2008). Seismic isolators are expensive in design, fabrication, and installation while the IDOT special thermal elastomeric bearing is relatively less expensive in those aspects. IDOT elastomeric bearing are Type I and Type II, which the first one has only soleplate and the second one has masonry plate and a PTFE surface to accommodate low friction. They also have some other detail to restraint them to move in transverse direction (Tobias et al. 2008). In Iran and some other countries, many bridges use thermal elastomeric bearing (Eshghi and Ahari 2005) with some differences to IDOT bearings and special seismic isolators. This type of bearing has no sole or masonry plate and without any bending requirements. This situation gives them the ability to slid on their seat (support length) while seismic isolators normally uses expensive bounding requirements to prevent them sliding and also unlike the IDOT bearings, it could rollover (Konstantinidis, Kelly, and Makris 2009a). Figure 1 (Kelly and Konstantinidis 2011) shows differences between bounded and unbounded elastomeric bearings' force-deformation behavior. The unbounded bearings experience a force cap in shear force which in, it could not bear excessive shear force increment because of friction force limit and consequently begin to slide. In bounded bearings, that cap doesn't exist, and its shear force increases with shear strain increment.

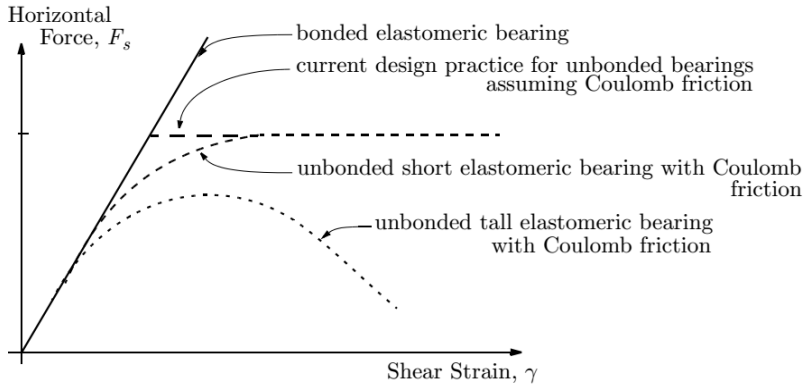

Figure 1. Behavior of bounded and unbounded elastomeric bearing (Kelly and Konstantinidis 2011).

Quasi isolated bridges get advantages of three- tier of redundancy defined to keep the bridge safe from earthquake demand. First-tier is elastic deformation and sliding of elastomeric bearing to cause quasi-isolation. Second-tier is providing sufficient support length to allow bearing sliding without bearing unsetting from provided support. The third tier is permitting substructure damage in so far as preventing span loss (LaFave et al. 2013). Generally, this method is defined as an IDOT earthquake resistance system (IDOT-ERS). Studies showed that the quasi isolation method could be chosen as a bridge earthquake design method (E. T. Filipov et al. 2011).

As a part of experimental and analytical studies of IDOT-ERS, some of them especially was on elastomeric bearing behavior. the experimental test has shown that elastomeric bearings can have exceptional performance, even under seismic loading (Steelman et al. 2011). Results show that 50% combined shear strain cap for elastomeric bearings, based on current design guidelines is overly conservative (Konstantinidis, Kelly, and Makris 2009a). Unbounded elastomeric bearings could deform in bigger shear deformation in a way which has been named roll-over, without significant damage. The elastomeric bearings roll-over takes place after 150% to 225% shear strain based on their heights and axial force. After that, the bearing could slide on its concrete seat with some abrasive damages to the elastomeric cap layer. It should be noted that after bearing roll-over, excessive expected soft shear deformation is locks and its shear stiffness rapidly goes up. It is assumed that shims will not yield and tear during roll-over (Kalfas, Mitoulis, and Konstantinidis 2020).

Despite additional experimental and analytical studies which are in demand for the quasi isolation design method, the previous researches showed that the friction coefficient between elastomeric bearing and its concrete seat could be an important part of the design (LaFave et al. 2013). The static and dynamic friction coefficient also considered in some researches (Evgueni T. Filipov et al. 2013), (Xiang et al. 2021). But the main problem is that for quasi-isolation design, laboratory test and control on elastomeric bearing and its seat condition goes minimum. So, due to variability in conditions (seat roughness, bearing axial force, bearing vax, weather deterioration, etc.), different friction coefficients are inevitable. Based on some other researches (Steelman et al. 2011; Roeder and Stanton 1992; McDonald, Heymsfield, and Avent 1999), this study used friction coefficient in three levels 0.20, 0.40, and 0.60 which seems to be a normal friction coefficient among those bridge elastomeric bearings which that coefficient mostly depend on bearing axial force and roughness of its concrete seat.

In this study, a designed elastomeric bearing that provides thermal and other design requirements for a two-span concrete bridge will go under some analytical study to show designers that considering affecting elastomeric parameters, plays an important role in quasi-isolation design. Hardness and after yielding stiffness of the bearing and the friction coefficient between elastomeric bearing and its concrete seat are among those parameters. Typically, in substructure elastic design for seismic actions, the thermal bearing stiffness is not considered and assuming a fixed connection between substructure and superstructure (AASHTO-LRFD 2012; Caltrans 2013). Considering the mentioned bearing stiffness will cause a softer structure which leads to a lower strong substructure. But when quasi-isolation functionality is expected from the bridge, bearing slip may cause bridge flexibility to increases even more. During a moderate to strong earthquake, the bearing slip is inevitable. This slip happens probably but in a different way. Unlike seismic isolators, thermal elastomeric bearing uses thin shims. These thin shims allow bearing to rollover for high shear deformation in relatively short

bearings. For tall bearing roll-off phenomena probably happens which is not this research case (Figure 2-e). So, as mentioned, two models of behavior may take place by shear deformation increasing. The first is hyper-elastic shear deformation, post-yield shear deformation and, bearing slip. The second is hyper-elastic shear deformation, post-yield deformation, rollover and immediately after, bearing slip (Figures 2-a to 2-d). Each model occurrence probability depends on bearing shear stiffness and friction coefficient. It should be noted that after rollover phenomena, excessive shear deformation is lock in bearing and only bearing slip is possible (Konstantinidis, Kelly, and Makris 2009b). The shear strain in rollover takes place as a function of geometric parameters of bearing and its axial load.

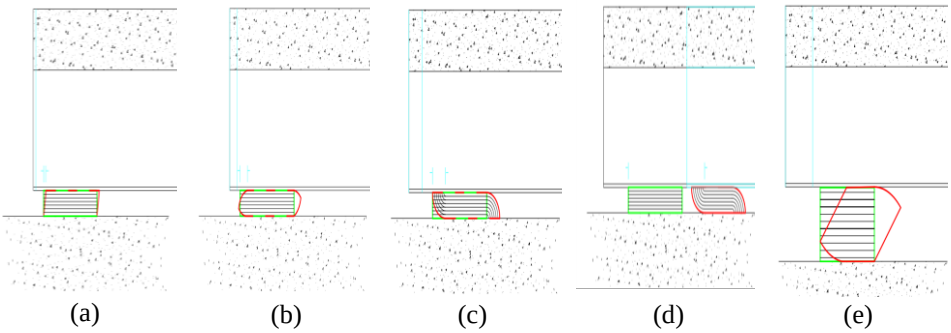

Figure 2. Sequence of elastomeric bearing shear deformation and slip, hyper-elastic deformation (a), the onset of bearing rollover (b), fully rollover bearing and shear locks (c), bearing slip (d), and bearing roll-off lead to bearing instability for tall bearings.

In this situation, the above-mentioned parameters (friction coefficient and bearing shear stiffness) play a key role in bearing behavior and consequently, have considerable effects on whole bridge seismic behavior (Wu et al. 2018).

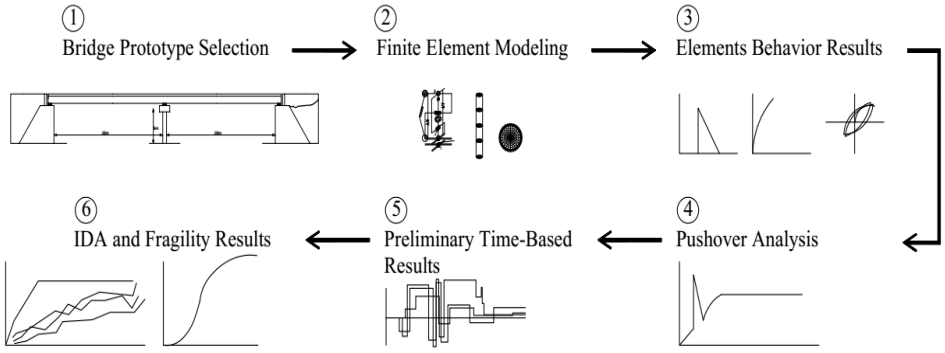

Figure 3. Schematic demonstration of the process of this research

In this research, the sensitivity of bridge deck displacement in the longitudinal direction to the mentioned parameters will study and the relevant pushover, IDA, and fragility curves will derive to illustrate the safety level of quasi-isolated bridge to deck unsetting. To clear this research path to its goal, Figure 3 presented the main elements of the research, graphically. Notably, bridge static and dynamic behavior in transverse and vertical directions have not been presented in this article.

2 PROTOTYPE BRIDGE DEFINITION

2.1 Geometry and material

A two-span highway concrete bridge with a middle multi-column pier is considered as the prototype bridge in this study. This type of bridge is the usual highway bridge type in Iran. Each span is 20m long with a 12m width continuous deck. The deck ends lay on abutment bearings and pier bearings in the middle. Abutments composed of the stem wall, backwall, and backfill soils which during earthquake resist against deck displacement in the longitudinal direction. Column pier consist of two column with 1200 mm diameter and their height is 5m. This bridge geometry is a typical highway bridge which traffic could pass under its spans and above on its deck. Figure 4 shows the main geometry of the bridge and Table 1 also presented the main feature of the bridge.

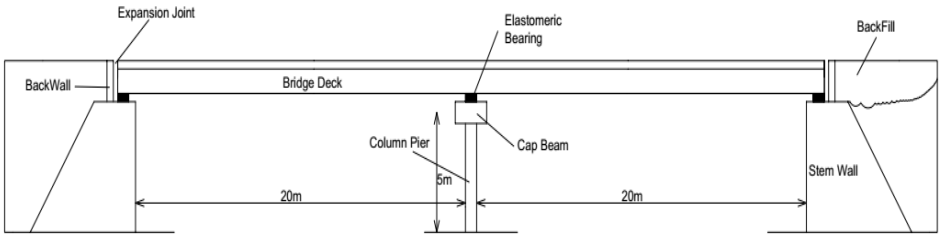

Figure 4. Schematic of prototype bridge section view and its details

The elastomeric bearing which is used in this study is a $300 \times 400\ mm$ square elastomeric bearing, normally used as a thermal bearing to accommodate thermal elongation of the bridge deck in the longitudinal direction. Rather than elastomeric pads which is a cut from an elastomeric volume, the mentioned bearing of this study is made up from layers of elastomer and thin steel shims to reinforce them. Eight 10mm layers of elastomer reinforced with seven 3mm layers of steel shims is the configuration of the bearing. Table 1 defines the basic properties of elastomeric materials which may be used in thermal bearings. Equations 1 to 4 define basic parameters which are the base for bearing behavior which is related to this table.

Table 1. Elastomeric material parameters.

	Hardness 50	Hardness 60	Hardness 70
E0 (MPa)	2.2	4.4	7.2
G (MPa)	0.68	1.04	1.69
k	0.73	0.57	0.53

Table 2. Main properties of prototype bridge.

Materials/Elements	Dimension/Properties			
Concrete	fc'=40 MPa			
Rebar	Yield stress 400 MPa, Ultimate Strength 500 MPa			
Column	Diameter:	1200 mm	Longitudinal bars:	Transverse Spirals:
	Height:	5000 mm	30T28 (rebar dia.=28 mm)	T14 @ 75 mm
Cap Beam	Height:	1200 mm	$I_x = 0.216\ m^4$	$I_y = 0.337\ m^4$
	Width:	1500 mm		
Abutment Back Wall	Width:	12000 mm	Longitudinal bars:	Transverse bars:
	Height:	1700 mm	T16 @ 300mm	T16 @ 300mm
	Thickness:	150 mm		
Elastomeric Bearing	Length:	300 mm	Elastomer:	Steel Shims:
	Width:	400 mm	8 layers	7 layers
	Height:	100 mm	Layer thickness: 10 mm	Layer thickness: 3 mm

$$S = {LW}/{2t_r(L+W)} \tag{1}$$

$$E_c = E_0(1 + 2kS^2) \tag{2}$$

$$K_v = E_c A/(nt_r) \tag{3}$$

$$K_h = GA/(nt_r) \tag{4}$$

In the above formulas, S is the shape factor, E_c is compression elastic modulus, and K_v and K_h are vertical and horizontal stiffness, respectively. L and W are the length and width of the elastomeric bearing. t_r is the thickness of a layer of elastomer and n is the number of them. A is elastomer area and E_0, G and k are parameters that are the basic properties of elastomeric material and have been defined in Table 1.

2.2 Minimum support length

In seat-type bridges, support length must accommodate expected bearing displacement demand from earthquakes and other loads. The support length must be able to prevent unseating and dropped spans/a. Span dropping was one of the dramatic bridge failure modes in past earthquakes while it is one of the easiest part of earthquake design. AASHTO, NCHRP and IDOT define N for 1000 years

return period earthquake as:

AASHTO $N = (8 + 0.02L + 0.08H)(1 + 0.000125S^2)$ (in) (5)

NCHRP & IDOT $N = [100 + 1.7L + 7.0H + 50\sqrt{1 + (2\frac{B}{L})^2}]\frac{(1+1.25F_vS_1}{cos\alpha}$ (m) (6)

Which in them, L, H and B are the length of the bridge deck to the adjacent expansion joint, bridge height, and bridge deck width, respectively. S is skewness and F_v, S_1 are seismic zone parameters. In this study the support length is calculated to be 670 mm, say 700 mm. it should be noted that for practice design, the pier cap width is considered twofold. For the abutment, seat width is measured from the center of the original location of elastomeric bearing to the edge of the seat but for the pier is the whole width of the cap beam as it's illustrated in Figure 5.

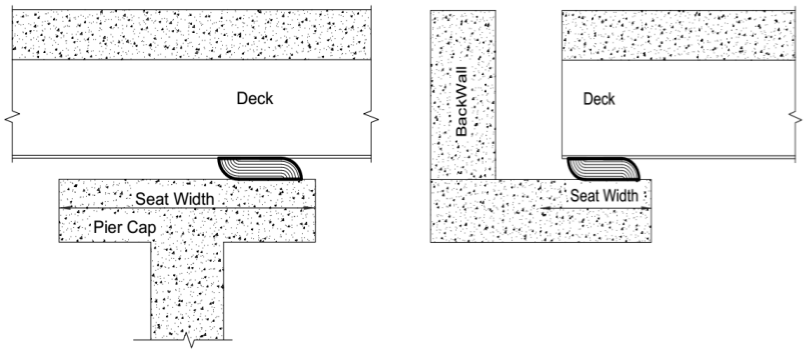

(a) (b)

Figure 5. Schematic Seat width definition on column pier (a) and abutment seat (b).

3 FINITE ELEMENT MODELING

In general, quasi isolated highway bridges are composed of three parts, substructure, superstructure, and the joint between them. When this configuration is selected as an ERS, mostly the superstructure remains elastic during earthquake, and damages to the substructure set to be minimum (U.S. Department of Transportation Federal Highway Administration 2014). But the joint between them is to consider how to probably suffer damages and goes beyond elastic behavior as a sacrificial element. In the quasi-isolation concept, the bearing mostly slid during moderate to strong earthquakes. Because of critical importance, the focus of this study is considerate on bearing deformation and slip which encompass tier 2 of IDOT ERS. So, superstructure is modeling elastic as in reality remains elastic in bridges with fusing system. OpenSEES (McKenna 2011) is used for finite element modeling. *elasticBeamColumn* element from the

OpenSEES library was used to model the bridge deck as an elastic beam. This is a beam-column element that could get the elastic properties of section and materials, therefore has linear behavior materially but, it could get geometric transformation nonlinearity. The grid deck method is used to model stiffness and mass distribution along widths and heights of the bridge deck using that element (Chang and White 2008; E. T. Filipov et al. 2011).

Substructure has two parts discluding foundations which here is assumed to be fixed. Those are column pier and abutments. The columns of multi-columns pier is modeled using a distributed plasticity *nonlinearBeamColumn* element (Neuenhofer and Filippou 1998). This element could get a predefined materially nonlinear section and geometric nonlinear transformation. Here, this element was employed in conjunction with the fiber section technique to apply nonlinear steel and concrete uniaxial materials as fibers of the section. Moreover, P-delta transformation is considered to model geometric nonlinearity. Each column element has five integration points and the Gauss-Lobatto integration method is used in them. *Steel02* and *Concrete04* were used as longitudinal bars and concrete fibers of the fiber section, respectively. *Steel02* is a uniaxial Giuffre-Menegotto-Pinto steel material object with isotropic strain hardening and Concrete04 is a uniaxial Popovics concrete material object with degraded linear unloading/reloading stiffness according to the work of Karsan-Jirsa and tensile strength with exponential decay. Figure 6 shows the column section and column element schematically.

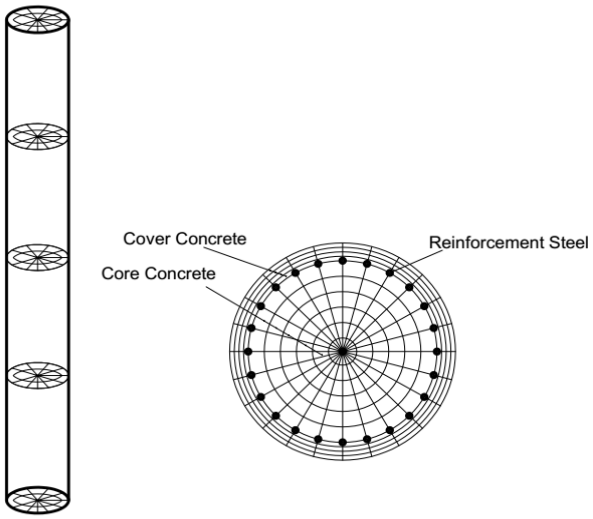

Figure 6. Schematic of column pier section and element integration points along with the element

For bearing modeling *elastomericBearingBoucWen* element in series with *flatSliderBearing* was used. The first bearing models thermal elastomeric bearing

and the second part models friction between elastomeric bearing and its concrete seat by defining the *Coulomb* friction model. Axial and shear stiffness of elastomeric bearing calculated using equation 1 to 4. Moreover, post-yield stiffness is considered to be 0.10 for all elastomer hardness. Friction coefficient in Table 3 defines the main factor of the Coulomb friction model. Figure 7 shows the general configuration of this modeling. It consists of two series elements which in elastomeric bearing element (between node 2 and 3), axial, shear, bending, and torsional springs have been defined. Moreover, an additional *twoNodeLinke* element connects node 2 and 3 to simulate shear lock behavior. The second element connects node 1 to node 2 and it simulates frictional behavior.

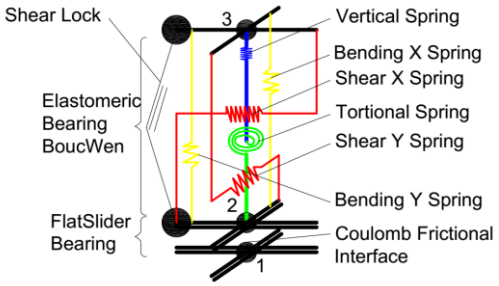

Figure 7. General configuration of bearing modeling

Table 3. friction coefficient used for sensitivity analysis

Friction coefficient
0.20
0.40
0.60

The Abutment is composed of a backwall that has a fixed shear connection to the stem wall and backfill which support them. Stem wall and back wall models using elastic beam-column elements with a nonlinear *twoNodeLink* shear connection between them that simulate backwall shear failure during deck pounding. Nonlinear backfill behavior under pressure also modeled using *q-z simple* soil model via a *twoNodeLink* element. It could not bear tensile force but behave nonlinear under pushing force. To model force transfer from deck to backwall, the *impact material* was used into a *twoNodeLinke* element (Zaghi et al. 2016; Omrani et al. 2015). This element material is a compression-only gap material that could get initial and secondary stiffness of transferring forces between deck and abutment.

4 BRIDGE ELEMENTS BEHAVIOR

To study the effect of elastomeric material hardness of thermal bearing in quasi-isolated bridges and the effect of friction coefficient between elastomeric bearing and its concrete seat, some static and many nonlinear dynamic analyses were performed. Generally, three grades of elastomeric hardness may use in thermal elastomeric bearings. As mentioned before, the quasi-isolation method has been defined to be a cheap method of design against expensive seismic isolator design

so, many laboratories test are excluded in the thermal bearing manufacture process. That's why the elastomer hardness may not belong to an exact hardness grade which led to different behavior due to hardness change. So, to simply demonstrate the hardness effect on bearing behavior, figure 8 demonstrated four different bearing behavior on various conditions.

Figure 8-a demonstrated a shear deformation behavior of a bounded bearing with different elastomer hardness. As it's clear, as a harder elastomer be used in bearing, a stiffer shear deformation could be expected from bearing. Even when the bearings are manufactured with the same elastomer hardness grade, the post yield stiffness (alpha) of elastomeric material may differ. Figure 8-b shows this phenomenon that its effect is the same as changing in elastomer hardness. So, these two phenomena categorized in the hardness effect group and the post yield of elastomeric bearing will not study independently. As mentioned before it consider to be 0.10.

Unbounded elastomeric bearing which is used in quasi-isolated bridges probably slid during moderate to strong earthquakes. Slide will happen when bearing shear force reaches to friction-resistant between bearing and its concrete seat. The amount of friction-resistant depends on bearing axial force and the friction coefficient. While the friction coefficient and axial force remains constant, horizontally stiffer bearing slid in lower shear deformation as illustrated in figure 8-c. after the resistant force and bearing shear force become equal, the bearing slid without any increase in shear force like the plateau line in the figure (friction coefficient in this model considered to be 0.20). It should be noted that after slid take place, static friction coefficient substitute with the dynamic friction coefficient which is a bit smaller (Steelman et al. 2011). But this switch is not what specifically this study intends.

As mentioned before, the real behavior of bearing in quasi-isolated bridges may lead to rollover and shear lock in higher shear deformations. The shear lock deformation depends on the axial load and bearing geometry which is not fully studied yet. But based on some researches (Konstantinidis, Kelly, and Makris 2009b; Kelly and Konstantinidis 2009), for bearing in this study we assume in an amount of 100 mm shear deformation, shear lock take place. After the shear lock, the bearing could not accommodate excessive shear deformation and acts like a relatively solid against further force. So, by force it in that direction, the shear internal force of it goes up rapidly. Figure 8-d demonstrated two bearing behavior. in the stiffer bearing (H50-alpha0.5 which mean a bearing made up of elastomeric material with hardness 50 and post-yield stiffness equal to 0.5) shear force reaches friction resistance before shear lock limit (100 mm) and begins to slide while the softer bearing (H50-alpha0.1) deform until reaches that limit whiteout slide. After that limit, shear deformation locks, and its shear force goes up rapidly to reach friction resistance, then starts to slide. This behavior is more realistic, and it have been derived from the proposed finite element model in figure 7 which is the base for this study.

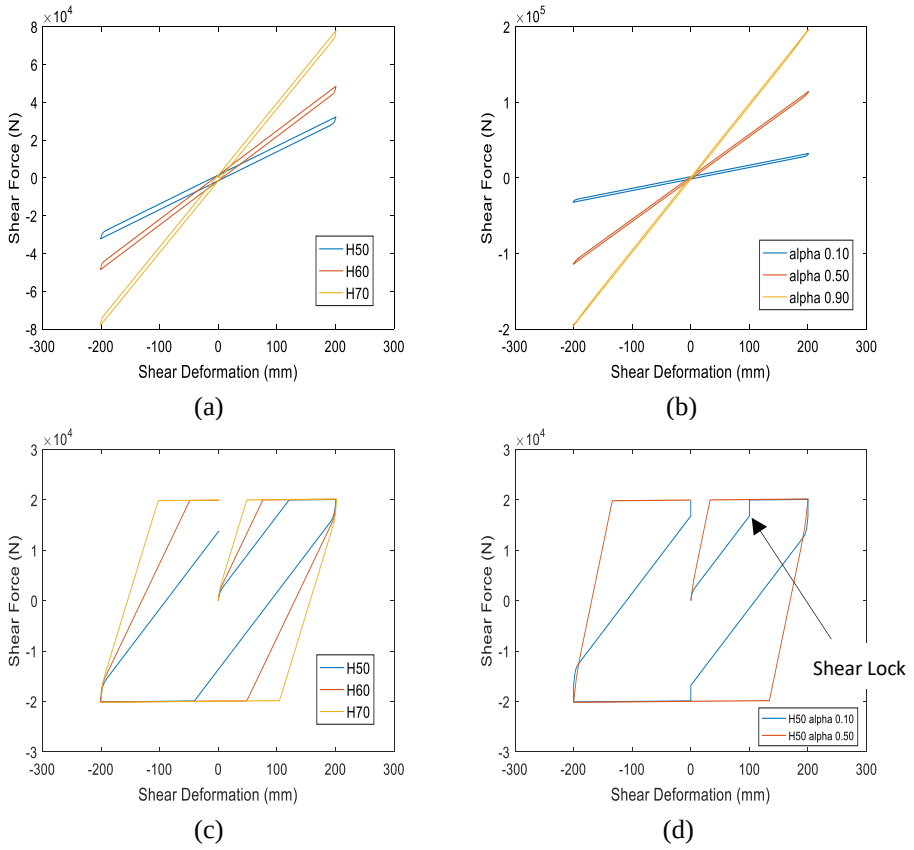

Figure 8. Elastomeric bearing behavior, bounded bearing behavior using different elastomeric hardness grades (a), effects of elastomeric post-yield behavior on bounded bearing (b), effects of elastomer hardness on unbounded bearing (c), and effects of bearing shear lock on the unbounded bearing

Dynamic behavior of elastomeric bearing may show more cycles of shear lock phenomena as illustrated in figure 9.

The distinguishing factor of this study was shear lock modeling for elastomeric bearings in quasi isolated bridges. Also, here there is no comparison between the results of bridges seismic analysis of other bearing modeling and this one, but Figure 9 demonstrate this study bearing behavior for different hardness and friction coefficients which in, bearing shear lock is bold. Those are bearing behavior on column pier under design earthquake (scale factor 1.0) of San Fernando (1971) ground motion record. Interestingly, the shear lock has happened for all hardness and friction coefficient conditions in design earthquake. The shear force cap is clear in the figures and the effect of shear lock which causes bearing to reach that cap rapidly and the onset of slip is clear as vertical lines. Obviously, Horizontal lines demonstrate bearing slip.

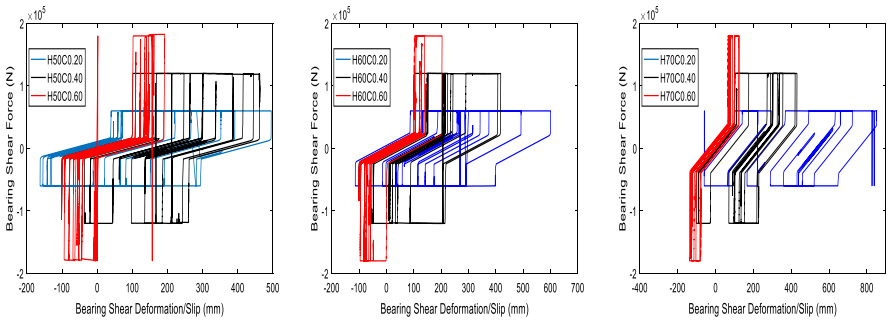

(a) (b) (c)

Figure 9. Bearing behavior on column pier for different hardness and friction coefficient under design earthquake (scale factor 1.0) of San Fernando (1971) ground motion record

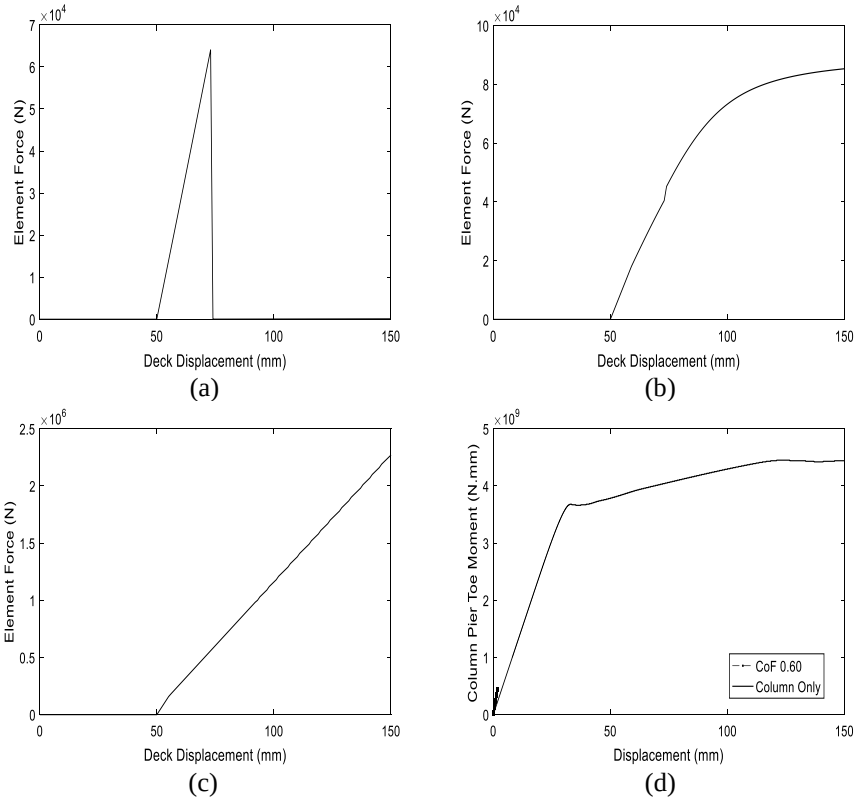

(a) (b) (c) (d)

Figure 10. Backwall (a), backfill (b), impact element (c) behavior and column pier in bridge model, lonely (d)

The predominant affecting element in quasi isolated bridges is elastomeric bearing. So, the main focus of this study was on that as described above but, for

clearness the backwall, backfill, impact, and column pier element monotonic behaviors also derived and presented in Figure 10.

As it clear in Figure 10-a backwall has a brittle behavior and backfill has curved behavior with a cap resistance force. Force transformation behavior of impact element also demonstrated in Figure 10-c. Figure 10-d shows the force deformation behavior of column pier which is mostly linear for a larger friction coefficient (Say 0.60). The column pier force deformation in the bridge model is compared with column force deformation alone. It is in the initial part of the elastic behavior of the column. So, it means that with this design, the column pier will not suffer damages and remain elastic because of its high strength (large section and short column length). So, the effects of column pier deformation will be minimum on bridge deck displacement.

5 NONLINEAR PUSHOVER ANALYSIS

Nonlinear pushover analysis was performed on three prototype bridge structure which in every model, the elastomer hardness of bearings was different, say 50, 60, and 70. Figure 11 shows the resistant force from a different element of substructure which resists against deck displacement and the total pushover curves.

Figure 11-a to 11-c shows those element shear reaction forces to deck displacement for hardness 50, 60 and 70 respectively. Those reactions consist of bearing and back wall reactions (B&B), column pier (CP), and backfill soil (BF). The A1 and A2 refer to abutment 1 and abutment 2. Despite bearings, backwall and backfill soil reaction start after expansion joint closure which is 50 mm. column pier reaction is higher than abutments reaction, because it takes higher axial force so, its friction force is higher. Interestingly, for grade 50 and 60 hardness, the bearings slip start at shear lock limit for both bearings (8-a and 8-b) while for grade 70 hardness, abutment bearing start to slid before that limit, and column pier bearings didn’t slide until that limit (8-c). Backwall has a brittle shear failure after reaches its ultimate strength. Commonly, the backwall fails in initial engagement with bridge deck because of its brittle manner. Backfill soil also reaches a steady reaction after backwall failure and enough deck displacement toward it.

Figure 11-d shows a comparison between those three models. Although the final reaction for all models is the same but, initial resistance to deck displacement differ. The model with higher hardness shows higher initial resistance. This difference will cause different dynamic behavior and different levels of safety that will be studies through incremental dynamic analysis (IDA) in the next section.

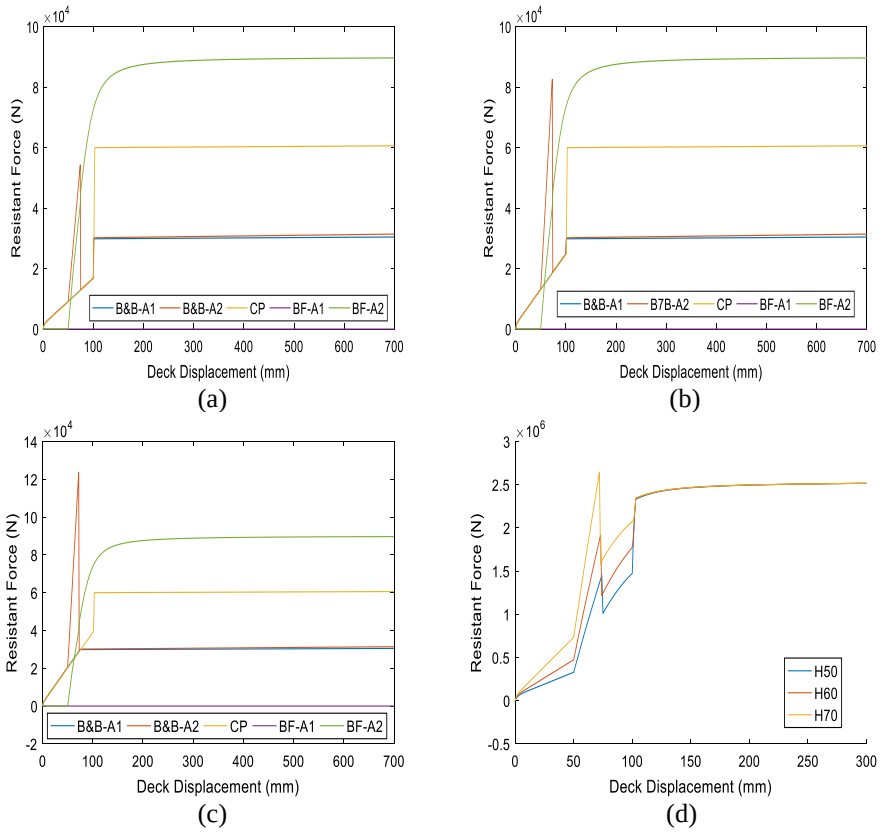

Figure 11. Bridge elements resistance to deck longitudinal displacement, (a) hardness 50, (b)hardness 60, (c) hardness 70 and (d) total pushover curve for all hardness levels

6 INCREMENTAL DYNAMIC ANALYSIS

6.1 Ground motion selection and scaling

IDA analysis (Vamvatsikos and Allin Cornell 2002) was performed on bridge models using a suit of 20 ground motion records. The ground motion records were selected from far-field records with magnitude from 6.5 to 7.5 and on soil type D. no fault type filter applied to the selection. Figure 12 shows the target spectrum for 1000 years return period earthquakes in Tehran which the mentioned ground motion records scaled to match that spectrum.

Each record scaled up and down using a defined scale factor which scales every 1000 years return period ground motions to 13 levels of magnitude from 0.25 to 1.75 in 0.125 steps. This scale factor will be used as an intensity measure to illustrate IDA results.

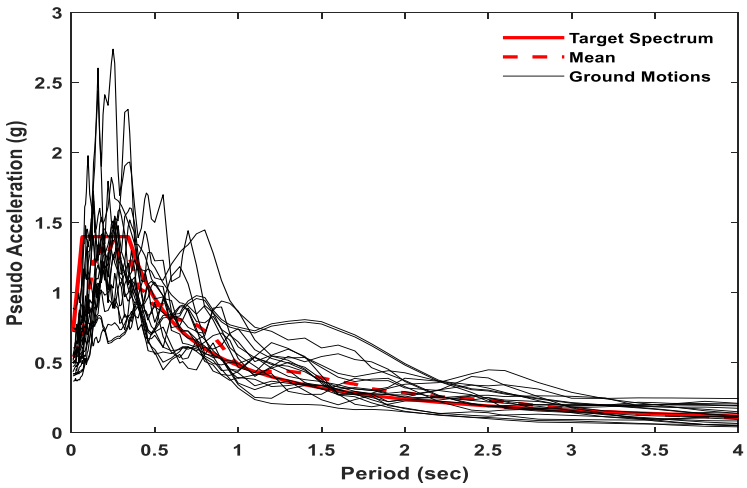

Figure 12. Spectrum of the selected ground motion compared with target and mean spectrum

6.2 Time-based results

Figure 13 show time history of bridge deck displacement and bearing slip in the longitudinal direction for three levels of elastomer hardness and different friction coefficients, under the San Fernando Earthquake record which its scale factor is 1. As mentioned before scale factor equal to 1 means design earthquake (DE) and a scale factor equal to 1.5 means maximum considered earthquake (MCE). As it's clear, it seems that for this specific ground motion record and for and 0.20 friction coefficient, harder bearing (hardness 70) shows larger displacement and bearing slip. Both pass 700 mm under design earthquake, which is the threshold of deck unsetting. It means the mentioned quasi isolated bridges are prone to experience deck unsetting as an unacceptable damage in all bridge design philosophies.

As AASHTO and Chinese Guidelines for Seismic Design of Highway Bridges recommend using 0.20 and 0.15 as the friction coefficient to assess the probability of deck unsetting respectively, it seems that using harder elastomer may worsen the situation. Figure 13 also shows that softer elastomers have smaller displacement and bearing slip under the same friction coefficient (0.20) and earthquake record.

As the friction coefficient rises, the deck displacement decreases for the same record and scale factor. Interestingly, the higher elastomer hardness (hardness 70) shows smaller fluctuation and displacement with a higher coefficient (0.40 and 0.60) of frictions in comparison with the 0.20 friction coefficient.

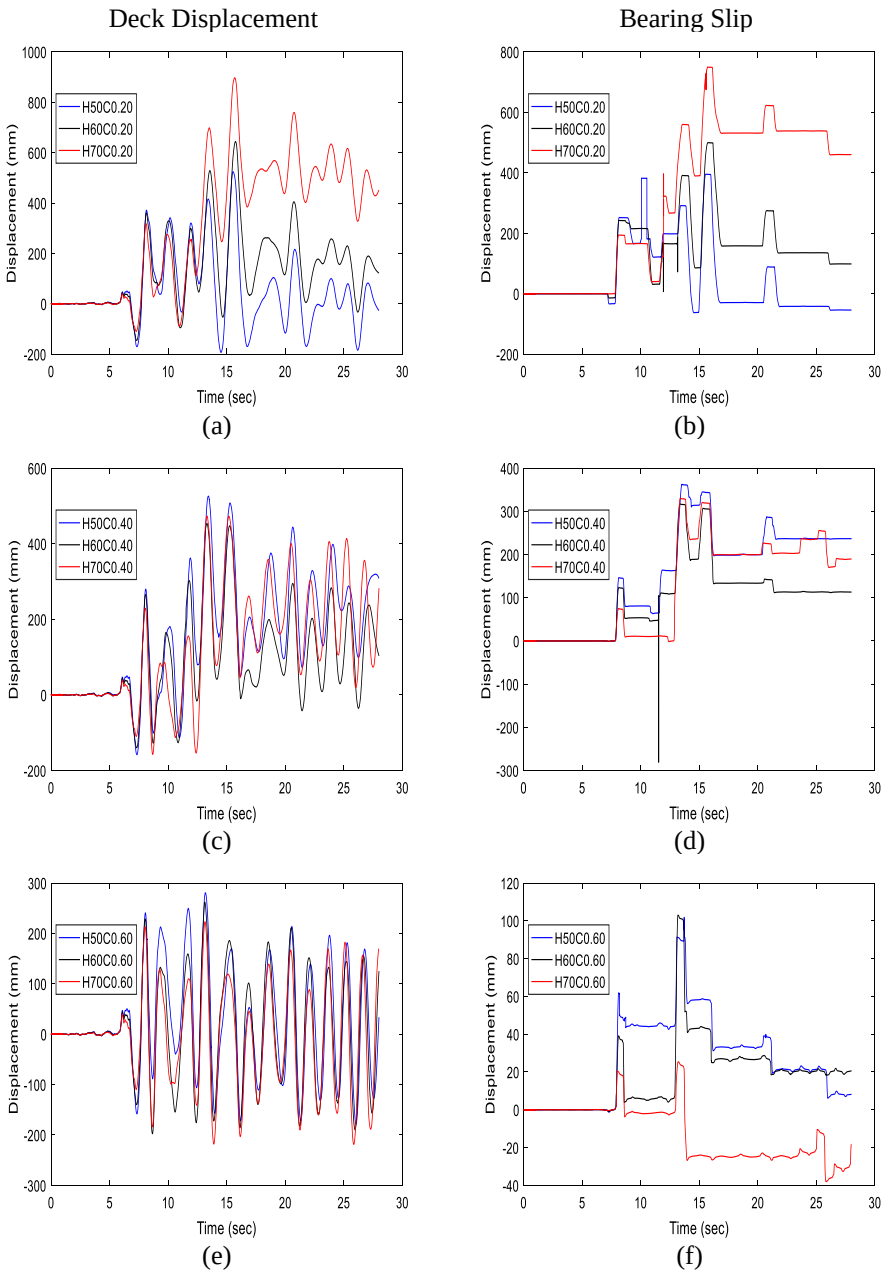

Figure 13. Bridge deck displacement (left) and Bearing slip (right) for different elastomer hardness under design earthquake (scale factor 1.0) of San Fernando (1971) ground motion record

To have a clearer view of the interaction between elastomer hardness and friction coefficient, Figure 14 shows bearing slip under the San Fernando ground motion

record for scale factor 1.0. All bearings with different hardness show lower slip with a friction coefficient rise. Figure 14-d shows deck slip for the same ground motion record as its magnitude rise. For scale factors equal to 0.25, 1.0, and 1.5 and bearing hardness 60 and friction coefficient 0.40, bearing slip behavior dramatically differs. It is near zero for scale factor 0.25 and scales factor 1.0 its maximum displacement increases to 300 mm. for scale factor 1.5 its maximum displacement hits 500 mm which is still in the safe border (less than 700 mm).

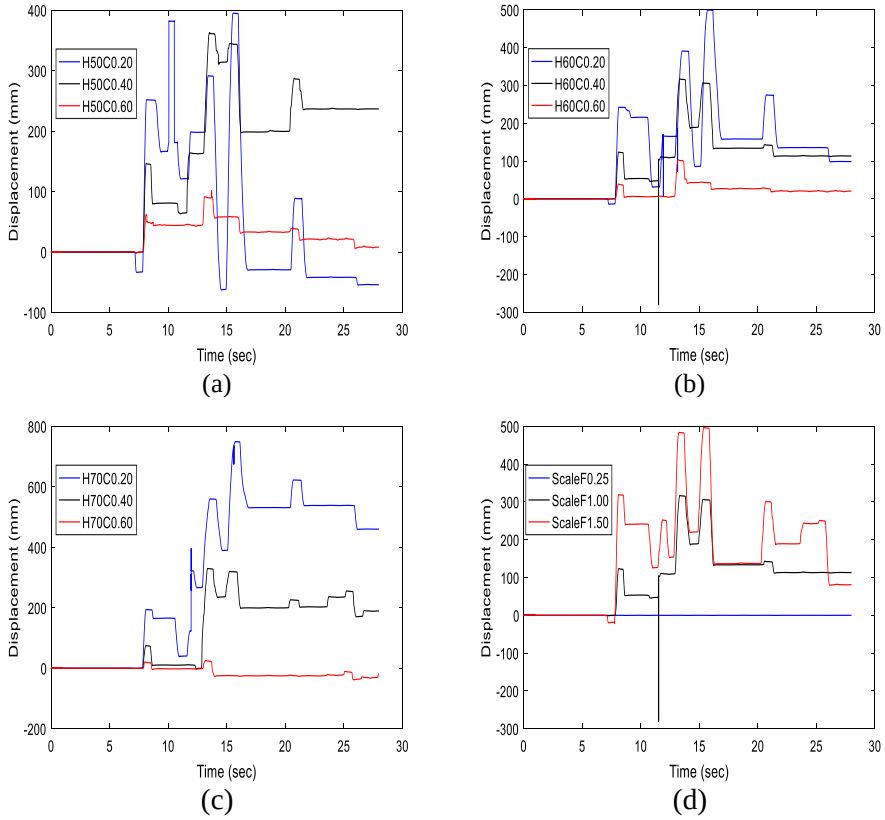

Figure 14. Bearing slip on column pier for the different friction coefficient under design earthquake (scale factor 1.0) of San Fernando (1971) ground motion record and effects of ground motion magnitude (*CoF* 0.40)

6.3 IDA and fragility

Figure 15 shows the mean of deck displacement for the ground motion records mentioned before. Moreover, the maximum and minimum standard variations for all bearing friction coefficient and elastomer hardness have presented. As a very early result of these figures, the friction coefficient has a more effective impact on mean deck displacement compared with elastomer hardness. By rising in friction coefficient, the mean deck displacement got smaller and with lower

differences due to hardness change under scale factor increasing. Figures show that for 0.60 friction coefficient deck unsetting would not happen while for 0.20 and 0.40 friction coefficient that probability exists. So, based on design codes, assuming 0.20 friction coefficient to calculate deck unsetting probability, a relatively high risk of deck unsetting could be proven based on this study. As it clear on figure 15-d (fragility curve), that probability could be up to 7 percent for hardness 50 and 11 percent for hardness 60 and 70 for design earthquake (scale factor 1.0) and 14 and 20 percent respectively for MCE (scale factor 1.50), which is relatively high risk for unacceptable damage like unsetting.

It should be noted based on the results of figure 15, deck displacement gets more than 50 mm for design earthquake and MCE in all conditions, so indirectly it could be inferred that backwall and backfill fail indefinitely.

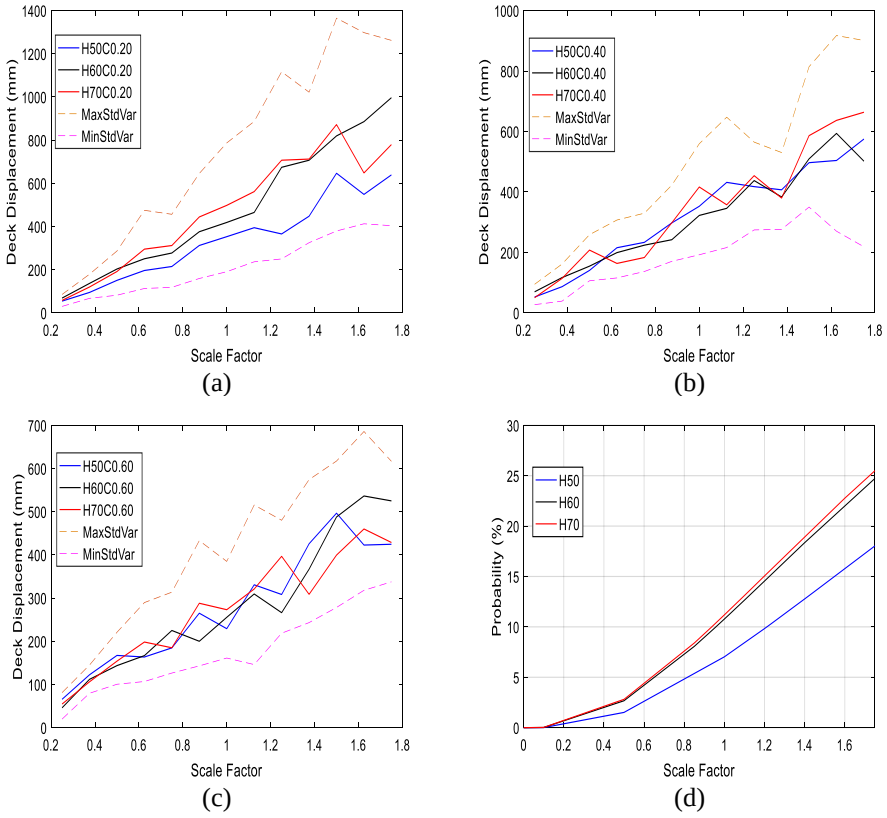

Figure 15. Deck displacement for different elastomer hardness and friction coefficient, (a): *CoF* 0.20, (b): *CoF* 0.40, (c): *CoF* 0.60 and (d) fragility curve for *CoF* 0.20

Figure 16 demonstrates curves of fixed hardness and varying *CoF*. In all cases, lower *CoF* caused larger deck displacement. Again, the curves show that an

increase in hardness will cause a higher risk of unsetting. Implicitly, the area between unsetting threshold line (700mm) and MCE and maximum standard deviation of deck displacement (hatched area) compared with the total area between MCE line and minimum and maximum line of standard deviation, is the probability of unsetting probability. This area is larger for hardness 70. This means that higher elastomer hardness has negative effect on quasi-isolated bridges' safety which increases the risk of deck unsetting.

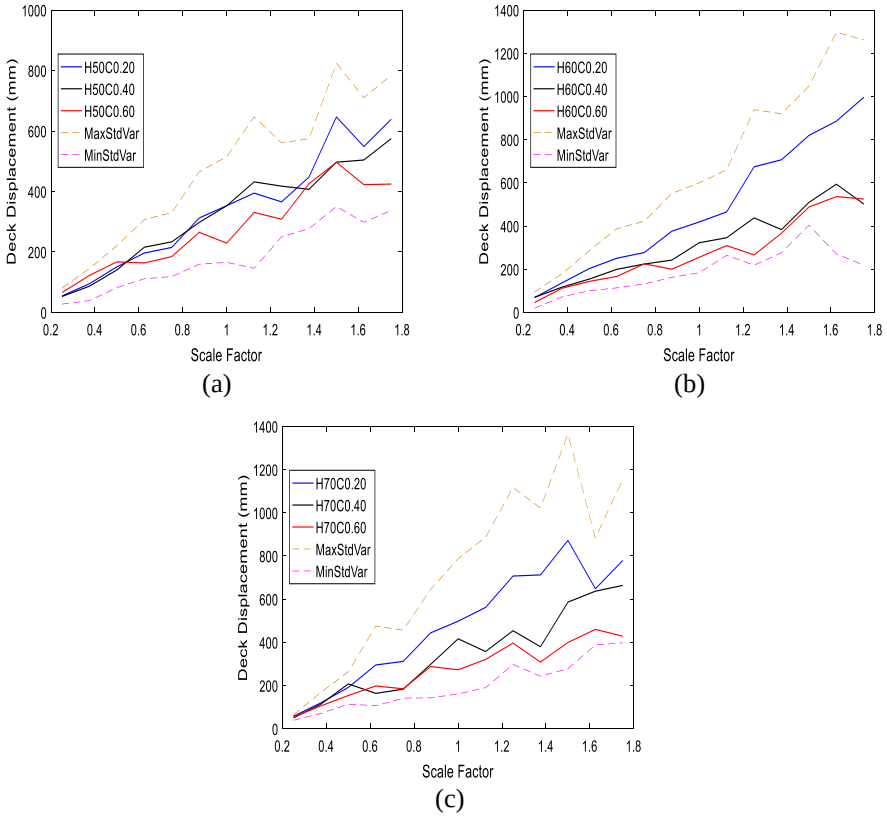

Figure 16. Deck displacement for fixed hardness and varying *CoF*, (a): Hardness 50, (b) hardness 60 and (c) hardness 70

One of the most important factors in bridge design is substructure strength design. It vitally depends on the amount of seismic demands which could pass through the fusing system between substructure and superstructure. Those demand in quasi isolated bridges are compression axial and shear forces. Due to the boundary condition of quasi isolated bridge bearing fabrication and installation, its bearing could not transfer tension or moment forces because it has not positive connection in those directions. So, the substructure column pier and other related

elements like foundation could be designed based on the maximum forces presented in Figure 17. It shows that the maximum shear force strongly depends on *CoF* and elastomer hardness has no effective impact on it. IDOT recommends using *CoF* 0.40 for substructure design but, based on this figure the worsen condition may arise from *CoF* of 0.60 or higher *CoF*s which may happen due to unstudied conditions (environmental, human error, and …) in this article. As it clear in figure 17-d and 17-e, axial force changes depend on seismic actions but, its changes are small (say one percent) compared to the initial gravity load.

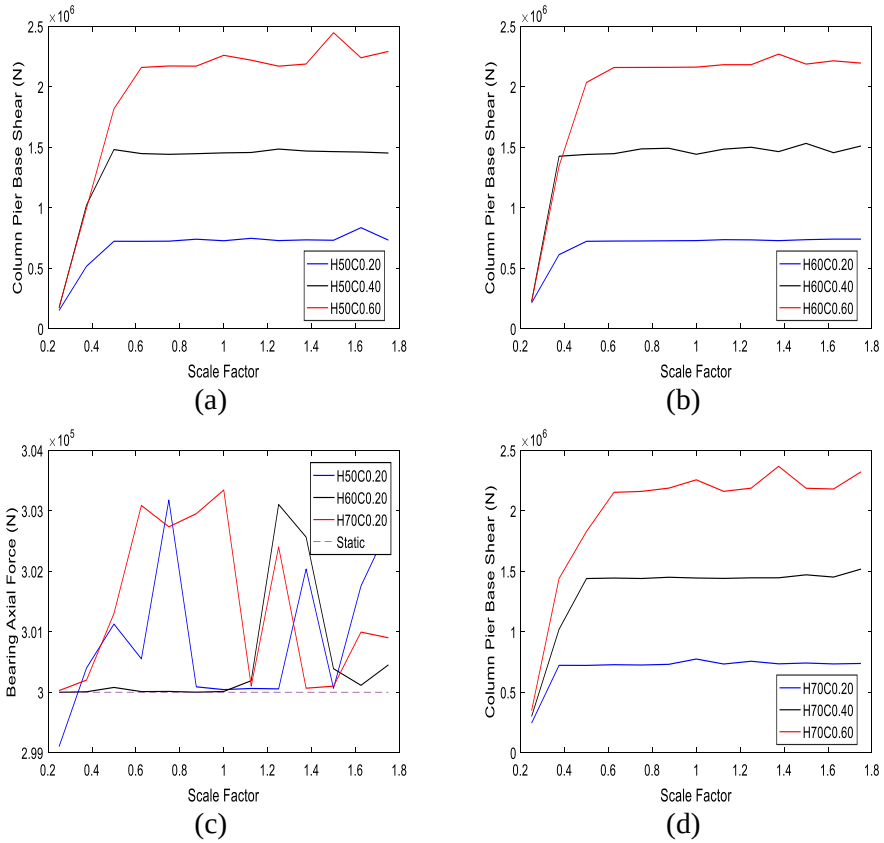

Figure 17. Column pier shear and axial force changes, (a) shear force for hardness 50, (b) shear force for hardness 60, (c) shear force for hardness 70, (d) axial force change in column pier bearing during design ground motion record San Fernando, (e) mean axial force changes for *CoF* 0.20

7 CONCLUSION AND RECOMMENDATION

A new approach is considered in finite element bearing modeling for quasi isolated bridges. That was considering shear lock phenomena in bearings due to rollover. Static pushover and nonlinear incremental dynamic analysis were conducted on a common quasi isolated highway bridge model. IDA performed

on bridge nonlinear model using a suit of 20 ground motion records which are selected using specific conditions. It was believed that CoF and elastomer hardness could affect the quasi isolated bridge deck unsetting safety in longitudinal direction under seismic loads so, results showed that:

1- Smaller CoF and larger elastomer hardness lead to a bigger probability of bridge deck unsetting in the longitudinal direction. Using elastomer with hardness 50 gives a safer condition under all *CoF*s and seismic actions.
2- The worst condition of unsetting was under *CoF* 0.20 which is AASHTO's recommendation to assess deck unsetting probability. The fragility curve derived for that condition showed that a nearly 10 percent probability of unsetting under design earthquake and up to 20 percent under MCE. These probability is derived based on support length calculated according to the AASHTO and IDOT support length formula which was here not more than 700 mm. because of the relatively high probability of deck unsetting for this quasi isolated bridge, it is recommended to use a larger support length than what calculate based on Codes. This means that Tier 2 of redundancy for quasi isolated bridge design, is not sufficient and must be modified.
3- Column pier gets seismic action mainly from bearing shear and axial forces. Shear force strongly depend on CoF which for *CoF* 0.60, the shear force is maximum. It's recommended to use a higher amount of *CoF* for substructure design sake, rather than what recommended in IDOT equal to 0.40. Axial force changes during an earthquake is very small (say one percent) so, considering gravity axial load in longitudinal direction seems safe enough for design's sake.
4- This study used only one bridge model and elastomeric bearing. It is recommended to use more geometrically different quasi isolated bridges and elastomeric bearing for future researches. Curved and skewed bridges with different levels of backwall and backfill strength may show a different level of unsetting safety.

8 DATA AVAILABILITY STATEMENT

Some or all data, models, or code that support the findings of this study are available from the corresponding author upon reasonable request.

REFERENCES

[1] AASHTO-LRFD. 2012. "AASHTO LRFD Bridge Design Specification, 6th Edition." *American Association of State Highway and Transportation Officials.*
[2] Bridges, Transportation Officials. Subcommittee on. 2011. *AASHTO Guide Specifications for LRFD Seismic Bridge Design*. AASHTO.
[3] Caltrans. 2013. "Caltrans Seismic Design Criteria Version 1.7." *California Department of Transportation: Sacramento, CA, U.S.*, no. April.
[4] Chang, Ching Jen, and Donald W. White. 2008. "An Assessment of Modeling Strategies for Composite Curved Steel I-Girder Bridges." *Engineering Structures* 30 (11).

https://doi.org/10.1016/j.engstruct.2008.04.011.
[5] Eshghi, Sassan, and Masoud N. Ahari. 2005. “Performance of Transportation Systems in the 2003 Bam, Iran, Earthquake.” *Earthquake Spectra*. https://doi.org/10.1193/1.2098891.
[6] Filipov, E. T., J. F. Hajjar, J. S. Steelman, L. A. Fahnestock, J. M. Lafave, and D. A. Foutch. 2011. “Computational Analyses of Quasi-Isolated Bridges with Fusing Bearing Components.” *Structures Congress 2011 - Proceedings of the 2011 Structures Congress*, 276–88. https://doi.org/10.1061/41171(401)25.
[7] Filipov, Evgueni T., Larry A. Fahnestock, Joshua S. Steelman, Jerome F. Hajjar, James M. LaFave, and Douglas A. Foutch. 2013. “Evaluation of Quasi-Isolated Seismic Bridge Behavior Using Nonlinear Bearing Models.” *Engineering Structures* 49 (April): 168–81. https://doi.org/10.1016/j.engstruct.2012.10.011.
[8] Kalfas, Konstantinos N., Stergios A. Mitoulis, and Dimitrios Konstantinidis. 2020. “Influence of Steel Reinforcement on the Performance of Elastomeric Bearings.” *Journal of Structural Engineering* 146 (10): 04020195. https://doi.org/10.1061/(asce)st.1943-541x.0002710.
[9] Kelly, James M., and Dimitrios Konstantinidis. 2009. “Effect of Friction on Unbonded Elastomeric Bearings.” *Journal of Engineering Mechanics* 135 (9). https://doi.org/10.1061/(asce)em.1943-7889.0000019.
[10] Kelly, James M., and Dimitrios A. Konstantinidis. 2011. *Mechanics of Rubber Bearings for Seismic and Vibration Isolation*. *Mechanics of Rubber Bearings for Seismic and Vibration Isolation*. https://doi.org/10.1002/9781119971870.
[11] Konstantinidis, Dimitrios, James M. Kelly, and Nicos Makris. 2009a. “Experimental Investigation on the Seismic Response of Bridge Bearings.” *International Conference on Advances in Experimental Structural Engineering* 2009-Octob.
[12] Konstantinidis, Dimitrios, James M. Kelly. 2009b. “Experimental Investigation on the Seismic Response of Bridge Bearings.” *International Conference on Advances in Experimental Structural Engineering* 2009-Octob (October).
[13] LaFave, James M., Larry A. Fahnestock, Douglas A. Foutch, J.S. Steelman, Jessica R Revell, Evgueni T. Filipov, and Jerome F. Hajjar. 2013. “Seismic Performance of Quasi-Isolated Highway Bridges in Illinois.” *Civil Engineering Studies Illinois Center for Transportation*, no. 13.
[14] McDonald, J, E Heymsfield, and R R Avent. 1999. “Investigation of Elastomeric Bearing Pad Failures in Louisiana Bridges.” Louisiana State University. Department of Civil and Environmental Engieering.
[15] McKenna, Frank. 2011. “OpenSees: A Framework for Earthquake Engineering Simulation.” *Computing in Science and Engineering* 13 (4): 58–66. https://doi.org/10.1109/MCSE.2011.66.
[16] Neuenhofer, Ansgar, and Filip C. Filippou. 1998. “Geometrically Nonlinear Flexibility-Based Frame Finite Element.” *Journal of Structural Engineering* 124 (6). https://doi.org/10.1061/(asce)0733-9445(1998)124:6(704).
[17] Omrani, Roshanak, Bahareh Mobasher, Xiao Liang, Selim Gunay, Khalid M Mosalam, Farzin Zareian, and Ertugrul Taciroglu. 2015. “Guidelines for Nonlinear Seismic Analysis of Ordinary Bridges: Version 2.0.” *Caltrans Final Report No. 15-65A0454*, no. December: 168. https://doi.org/10.13140/RG.2.1.4946.6648.
[18] Roeder, Charles W., and John F. Stanton. 1992. “Steel Bridge Bearing Selection and Design Guide.” *Highway Structures Design Handbook* 2.
[19] Steelman, J. S., L. A. Fahnestock, J. M. Lafave, J. F. Hajjar, E. T. Filipov, and D. A. Foutch. 2011. “Seismic Response of Bearings for Quasi-Isolated Bridges- Testing and Component Modeling.” *Structures Congress 2011 - Proceedings of the 2011 Structures Congress* 41171 (April): 164–78. https://doi.org/10.1061/41171(401)16.
[20] Tobias, Daniel H., Ralph E. Anderson, Chad E. Hodel, William M. Kramer, Riyad M. Wahab, and Richard J. Chaput. 2008. “Overview of Earthquake Resisting System Design and Retrofit Strategy for Bridges in Illinois.” *Practice Periodical on Structural Design and Construction* 13 (3): 147–58. https://doi.org/10.1061/(ASCE)1084-0680(2008)13:3(147).

[21] U.S. Department of Transportation Federal Highway Administration. 2014. “LRFD Seismic Analysis and Design of Bridges - Reference Manual,” no. FHWA-NHI-15-004: 608.

[22] Vamvatsikos, Dimitrios, and C. Allin Cornell. 2002. “Incremental Dynamic Analysis.” *Earthquake Engineering and Structural Dynamics* 31 (3): 491–514. https://doi.org/10.1002/eqe.141.

[23] Wu, Gang, Kehai Wang, Guanya Lu, and Panpan Zhang. 2018. “An Experimental Investigation of Unbonded Laminated Elastomeric Bearings and the Seismic Evaluations of Highway Bridges with Tested Bearing Components.” *Shock and Vibration* 2018. https://doi.org/10.1155/2018/8439321.

[24] Xiang, Nailiang, Yoshiaki Goto, M. Shahria Alam, and Jianzhong Li. 2021. “Effect of Bonding or Unbonding on Seismic Behavior of Bridge Elastomeric Bearings: Lessons Learned from Past Earthquakes in China and Japan and Inspirations for Future Design.” *Advances in Bridge Engineering* 2 (1). https://doi.org/10.1186/s43251-021-00036-9.

[25] Zaghi, Arash E., Siavash Soroushian, Alicia Echevarria Heiser, Manos Maragakis, and Amvrossios Bagtzoglou. 2016. “Development and Validation of a Numerical Model for Suspended-Ceiling Systems with Acoustic Tiles.” *Journal of Architectural Engineering* 22 (3): 1–13. https://doi.org/10.1061/(ASCE)AE.1943-5568.0000213.